Eur. Phys. J. B **38**, 71–82 (2004)
DOI: 10.1140/epjb/e2004-00101-6

THE EUROPEAN PHYSICAL JOURNAL B

From weak to strong pinning I: A finite size study

A. Tanguy[a] and T. Vettorel

Laboratoire de Physique de la Matière Condensée et des Nanostructures, Université de Lyon I,
43 boulevard du 11 Novembre 1918, 69622 Villeurbanne, France

Received 3 February 2003 / Received in final form 12 September 2003
Published online 20 April 2004 –

Abstract. We have used linear stability analysis to study the depinning of an elastic chain with long range interactions submitted to a random pinning potential. In this paper, we provide, for the first time, evidence of a pronounced change from a strong pinning regime to a weak pinning regime. This change depends on the strength of disorder, and takes place only in finite size systems. For a given disorder, we show a characteristic length separating the weak pinning regime from the strong pinning regime. This length depends on the long range of the algebraic decay of the elastic couplings. The weak pinning regime is very well described by perturbation theory. As an example, we discuss more specifically the case of wetting of heterogeneous surfaces, where the change from a strong to a weak pinning regime could be induced in the wetting front by varying the surface tension of the liquid-air interface.

PACS. 05.10.-a Computational methods in statistical physics and nonlinear dynamics – 68.08.Bc Wetting – 02.50.Fz Stochastic analysis

1 Introduction

Pinning of elastic media can be used to describe various physical situations such as roughening of crack front in fracture [1,2], wetting front motion on heterogeneous surfaces [3–16], dynamics of a ferromagnetic domain wall driven by an external magnetic field [21], motion of vortices in type-II superconductors [22], or even solid friction [23–28]. In all of these cases, the complex dynamics of the system results from the competition between an elastic restoring force (such as capillary forces in wetting) and a non-linear pinning force (due to heterogeneous contact surfaces for example). The latter contribution is often described by a quenched, time-independent, disorder term that gives rise to a so-called *deterministic* noise. This noise is part of the permanent forces acting on the system, even at zero temperature. It is not a thermal noise. It has been shown [29] that this zero temperature noise cannot be mapped to a simple Langevin force, but is responsible for memory effects [30], giving rise to a situation that cannot be described simply by the usual statistical theory [30] (due to temporal correlations). One crucial point is indeed to understand in which order the system reaches or leaves the successive equilibrium positions, taking into account the external deterministic driving.

Various theoretical approaches have thus been proposed to describe the stationary state of an elastic medium driven quasistatically at zero temperature in a random potential. Perturbation and variational theories used in references [5,20,22], or renormalisation group calculations [16–19] consider the disorder term as a perturbation. This should a priori correspond to a situation where the pinning is *weak*, and the straight line is then usually chosen as a reference state. In numerical studies on the contrary [15,31], the disorder is *strong* in order to allow the use of local algorithms such as cellular automata. The resulting stationary state of the elastic system is not the same in both cases. In the *strong* pinning case, the dynamics of the system, when it is driven, is localized around very few pinning centers. But in the *weak* pinning case, the system may advance as a whole. More phenomenological studies propose to describe the elastic system driven on the pinning surface as a set of blocks advancing coherently. This description was first proposed by Larkin and Ovchinninkov [22] in the context of type-II superconductors. One of the very interesting consequences of this description was the ability to relate the critical current of the superconductors to the size of the correlated volume taking place in the elastic lattice of flux lines. This kind of description has also been used in the context of solid friction [23–27] but without any strong experimental evidence. Finally, Joanny and Robbins [13] have proposed to describe the stationary state of the system as a set of blocks *weakly* pinned at small scales (where elasticity would be dominant) but *strongly* pinned at large scale (where disorder would dominate). The characteristic size separating the two regimes would correspond precisely to

[a] e-mail: atanguy@lpmcn.univ-lyon1.fr

the Larkin length [22] of the *correlated* volume, and each regime would be characterized separately by a roughness exponent. Originally, the Larkin length [22] is defined as the characteristic length beyond which the fluctuations of the displacement field become larger than the typical size of a pinning center. Nowadays, it is not clear whether such a correlation volume would result from finite temperature effects as in reference [20], or from the deterministic dynamics of the elastic medium on the disordered surface.

In this paper, we study the case of a one-dimensional elastic line driven at zero temperature on a pinning surface. One related physical situation is the case of wetting of heterogeneous surfaces, where the elastic line is the contact line and the disorder is due to chemical heterogeneities or to the roughness of the heterogeneous solid substrate [3–7]. Depending on the geometry of the system (free surface or Hele-Shaw cell [3,33] for example), the elastic couplings may be long-range or short-range [3]. In the following, we will use the exponent of the algebraic decay of the couplings as a parameter. The size of the system (or the density of the pinning centers) will be another parameter, as well as a dimensionless parameter G characterizing the surface tension to pinning ratio. We do not consider here the possible role of anisotropy [32], since each point of our line is allowed to advance only in the perpendicular direction. For sake of simplicity, the possibility of surrounding the defects in wetting [33], is thus not allowed here.

The questions we address are: Is it possible to define properly a characteristic change from a *weak* pinning to a *strong* pinning regime? How does this change depend on the control parameters listed above? And does the critical size correspond particularly to the Larkin length?

In order to answer those questions, we have done a stability analysis of our system. It is now well known that, when it is driven quasistatically, an elastic system can display instabilities [3–7,18,23–28] during which it dissipates energy [3,23]. This is one of the manifestations of its possible multistability: the system goes from one local equilibrium position to another, following an out-of-equilibrium path. In the case of wetting of heterogeneous surfaces, this dissipation of energy is related to the well known *hysteresis* of the contact angle [3–7]. Few authors [22–25] have proposed to relate the size at which the system becomes unstable to the Larkin length. Experimentally, it has been shown that the hysteresis of the contact angle depends strongly on the density of the pinning centers [6–8], with a regime at very low density where each center contributes independently to the hysteresis, and a non-linear regime at higher densities that can be explained only by collective effects. However, despite isolated claims [13,22,23], the critical density (or critical size) at which this transition occurs has never been related precisely to a characteristic length along the wetting front itself. The morphology of the contact line has been measured by several groups [9–12], giving rise to a description in terms of roughness exponent. In this paper, we will compare the morphology of the line, when it becomes unstable, to the characteristic size at which instability occurs.

The paper is organized as follows: In Section 2, we will define our system and describe the stability analysis used as a starting point of our study. In Section 3, we will provide numerical evidence of a pronounced change from a weak to a strong pinning regime and characterize the morphology of the line in both regimes. We will also study numerically the finite-size dependence of this transition. In Section 4, we present a perturbative calculation whose results are in very good agreement with those obtained numerically in the weak pinning regime. Section 5 is devoted to the conclusion.

2 Instability criterion

In case of the spreading of a liquid on a solid surface [3,4], pinning comes from the inhomogeneities of the contact surface. In this case, the solid-vapor and the solid-liquid surface tensions are modulated in space and the pinning energy may be written as

$$V_p = -\int_0^L dx \int_0^{u(x)} dy \; (\gamma_{SV}(x,y) - \gamma_{SL}(x,y)) \qquad (1)$$

where $\gamma_{SV}(x,y)$ and $\gamma_{SL}(x,y)$ are spatially varying solid-vapor and solid-liquid surface tensions, L is the size of the contact line, and $u(x)$ its position on the pinning surface (see Fig. 1). Another energy term comes from the increase of the area of the liquid-vapor interface due to the distortions of the contact line. Together with the gravitational energy, this gives rise [6] to a long range elastic force along the front, acting on x:

$$F_{el}(x,u(x)) = -\mathcal{G}\int_{|x-x'|\geq d}^{L} dx' \, \frac{u(x)-u(x')}{|x-x'|^{\alpha}} + Ku(x), \qquad (2)$$

where the first term on the right hand side is the translationally invariant component, and $Ku(x)$ is the remainder. The exponent of the algebraic decay, α, corresponds to $\beta+1$ of references [16–19] where the elastic couplings are defined in the Fourier space, for $1<\alpha<3$. The case $\alpha<1$ gives rise to large scale singularities, in which case equation (2) can be rewritten as $K'(L,\alpha)\,(u(x)-\langle u\rangle)+Ku(x)$. This corresponds to the mean field case studied in the next paragraph, but with the stiffness $K'(L,\alpha)$ dependent on the size. d is a small distance cut-off that we will choose to be equal to the distance between pinning centers, and in the special case of wetting [6]

- $\alpha=2$ and $\mathcal{G}=\gamma L\sin^2\theta/\pi$, if $d<|x-x'|<\kappa^{-1}$ (κ^{-1}, capillary length)
- $\alpha=0$ and $\mathcal{G}=\gamma\kappa\sin^2\theta$, if $\kappa^{-1}<|x-x'|<L$.
- Laplacian couplings (or equivalently harmonic nearest neighbour couplings in discrete systems) in a Hele-Shaw cell [3,33] where the liquid is confined between two plates, at distances larger than the thickness of the cell.

Note that in other cases of pinning of elastic media like in crack propagation [1], the term $Ku(x)$ can be ignored.

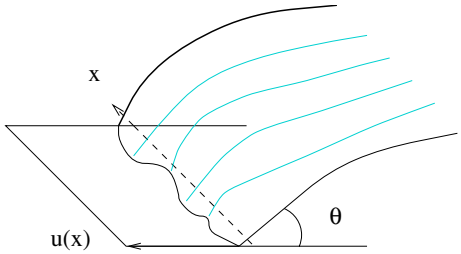

Fig. 1. Geometry of wetting. $u(x)$ is the position of the contact line on the pinning surface. We use periodic boundary conditions in the x-direction.

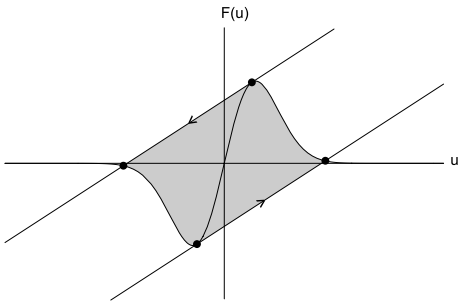

Fig. 2. Graphical construction of the equilibrium position u_{eq} in the one defect case. The gray area is the hysteresis cycle corresponding to the hysteresis of contact angle in wetting.

As will be seen later, it contributes only to the average (mean field) motion of the front. We will thus denote as *elastic* forces only the translationally invariant term in equation (2). The remainder will be included in the *external* driving. Note also that the case of a purely constant external driving (with stiffness zero) is meaningless in practical situations. Assuming that the motion of the contact line is overdamped, the equation of motion thus reads

$$\eta\frac{\partial u(x,t)}{\partial t} = -\frac{\partial V_p\big(x,u(x,t)\big)}{\partial u} - \mathcal{G}\int_d^L dx' \frac{u(x,t)-u(x',t)}{|x-x'|^\alpha} + F_{ext}(u(x,t),t). \quad (3)$$

A quasi-static solution $u_{eq}(x,t)$ is given by the condition $\partial u(x,t)/\partial t = 0$. Unlike any equilibrium position, the quasi-static solution results from a given succession of equilibrium positions [34], depending on the driving mode. In the following, we will see how the contact line departs from its initial equilibrium position, in a quasi-static way.

Let us first study the instructive case of a rigid line driven at velocity v by a spring of stiffness λ. The corresponding equations are the same as in the well known case of a single defect [3,7], because in this case the elastic force applied by the line on the defect is simply proportional to the distance between the defect and the position of the line at large distances. It is characterized by a constant stiffness. This situation also corresponds to the *mean field* case studied in reference [18]. In these cases, equation (3) reads

$$\eta\frac{du}{dt} = -V_p'(u) + \lambda(vt-u). \quad (4)$$

The quasi-static solution u_{eq} is given by

$$-V_p'(u_{eq}) + \lambda(vt-u_{eq}) = 0. \quad (5)$$

It can be solved graphically as in Figure 2 where $F(u) \equiv -V_p'(u)$. When the stiffness λ is weak, the solution is multivalued. The solution u_{eq} becomes unstable when the stiffness λ and the tangent to the pinning force are equal, that is

$$V_p''(u_{eq}) + \lambda = 0. \quad (6)$$

This corresponds to the spinodal limit, after which the system will follow an out-of-equilibrium path and dissipate energy before it reaches the next stable equilibrium position. In wetting, the energy dissipated during a complete cycle corresponds to the macroscopic hysteresis of the contact angle [3,7].

In the general case of a deformable line on many defects, the instability criterion (Eq. (6)) is obtained by a linear stability analysis. Starting with an equilibrium configuration (or quasi-static solution) $u_{eq}(x,t)$, we can ask whether a small perturbation $\delta u(x,t) \equiv u(x,t) - u_{eq}(x,t)$ would be amplified with time. Writing

$$\delta u(x,t) = \delta U(x) e^{-\omega t} \quad (7)$$

and using equation (3), we get to the first order in δU

$$\eta\omega\delta U(x) = \frac{\partial^2 V_p\big(u_{eq}(x)\big)}{\partial u^2}\delta U(x) + \mathcal{G}\int_d^L dx' \frac{\delta U(x)-\delta U(x')}{|x-x'|^\alpha} + K_{ext}\delta U(x). \quad (8)$$

where $K_{ext} \equiv -\partial F_{ext}(u_{eq}(x))/\partial u$ is the external stiffness – eventually taking into account the non-translationally invariant part of $F_{el}(x)$ (Eq. (2)). Equation (8) can be solved easily by discretizing the line in N sites x_i with $Nd = L$. We get for each site

$$\eta\omega\delta U(x_i) = \Sigma_j \mathcal{A}_{ij}\delta U(x_j) \quad (9)$$

where $\mathcal{A}_{ij}$ are the coefficients of the dynamic matrix $\mathcal{A}$

$$\mathcal{A}_{ii} \equiv \frac{\partial^2 V_p\big(u_{eq}(x_i)\big)}{\partial u^2} + \mathcal{G}\sum_{j=1}^{N} d\frac{1}{|x_i-x_j|^\alpha} + K_{ext} \quad (10)$$

$$\mathcal{A}_{ij} \equiv -\mathcal{G}d\frac{1}{|x_i-x_j|^\alpha}, \text{ for } i \neq j.$$

ω and $\delta U(x)$ are an eigenvalue and the associated eigenvector of $\mathcal{A}$ respectively. $\delta U(x)$ characterizes the shape of the line when it relaxes to its equilibrium position ($\omega > 0$), or when it leaves its equilibrium position ($\omega \leq 0$). ω is the inverse of a relaxation time. $-\omega\delta U(x)$ is the velocity field of the instability. In this paper, we will consider only the most unstable mode (i.e. with the largest relaxation time). We thus restrict our study to the minimum eigenvalue ω_{min} of $\mathcal{A}$. For a given u_{eq}, the instability corresponds to

$$\omega_{min} \leq 0. \quad (11)$$

In the following, we solve equation (9) numerically by using the exact diagonalization recursive scheme EISPACK [35] in Fortran. For large sizes ($N > 64$) we use the ARPACK algorithm and its parallel version PARPACK [36] based on the Arnoldi Approximation. Pinning forces are chosen randomly: $V_p''(u_{eq})$ is a random white noise [37] of zero mean between $-1/2$ and $+1/2$ whose variance W is fixed ($W = 1/\sqrt{12}$). The dimensionless parameter characterizing the elasticity to pinning ratio is

$$G = \mathcal{G}d^{1-\alpha}/W.$$

We call this the *dimensionless surface tension*. Large disorder would correspond to small G. We will now show how the characteristics of the instability depend on G, as well as on the system size N.

3 From weak to strong pinning

Let us first vary the dimensionless surface tension G. In the limit $G \to \infty$ the line is infinitely rigid and moves as a whole. Equation (6) holds for the whole line with the average pinning $\langle V_p'' \rangle$. In the opposite limit $G \to 0$, each site moves independently and equation (6) holds, but for each site independently. In this case, the eigenvector of $\mathcal{A}$ associated with the smallest eigenvalue ω_{min} is thus peaked around the site x_{i0} with the smallest $V_p''(x_{i0})$. This situation corresponds to the *strong* pinning case, while the former case is the *weak* pinning limit. To study the change from the strong to the weak pinning regime, it is useful to consider the participation ratio

$$\tau = \frac{1}{N} \frac{\left(\sum_{i=1}^{N} \left(\delta U(x_i) \right)^2 \right)^2}{\sum_{i=1}^{N} \left(\delta U(x_i) \right)^4}. \qquad (12)$$

The parameter τ measures the relative number of sites implied in an instability. In the *strong* pinning limit where only one site moves, we get $\tau = 1/N$. In the *weak* pinning limit, where $\delta U(x_i) \propto 1/\sqrt{N}$, $\tau = 1$. This parameter τ has also been used in the study of localization [38]. We will use it here to study the change from the *strong* to the *weak* pinning regime. For a given configuration of the disorder, we compute numerically $\tau(G)$. The result is shown in Figure 3 for $N = 128$ and for various couplings α. We show clearly in this figure a well-defined transition between the *strong* pinning regime (at small G) and the *weak* pinning regime (for large G). For each configuration, the critical G_c is uniquely defined as the maximum of the derivative $d\tau(G)/dG$. We see also in this figure that G_c is an increasing function of α for a given size N and a given configuration: this means that for long range couplings it is easier to reach the *weak* pinning regime than for short range couplings. But it is difficult to give more quantitative results at this stage, because G_c varies strongly from one configuration to the other.

We have thus studied more precisely the statistical distribution of G_c and its dependence on the system size, for various integer couplings α. We plot in Figure 4 the distribution of the critical value G_c of the transition. This figure has been obtained with 5 000 different configurations of disorder. We see that for $\alpha \leq 1$ the transition is very well defined for large size systems ($N > 128$). In contrast, for $\alpha > 1$, the distribution becomes larger as the system size N increases. As can be seen in Figure 5, the variance of the distribution increases exponentially with the system size. Thus the change from the *strong* to the *weak* pinning depends strongly on the configuration of disorder when the elastic couplings are short range ($\alpha > 1$), even for large system sizes.

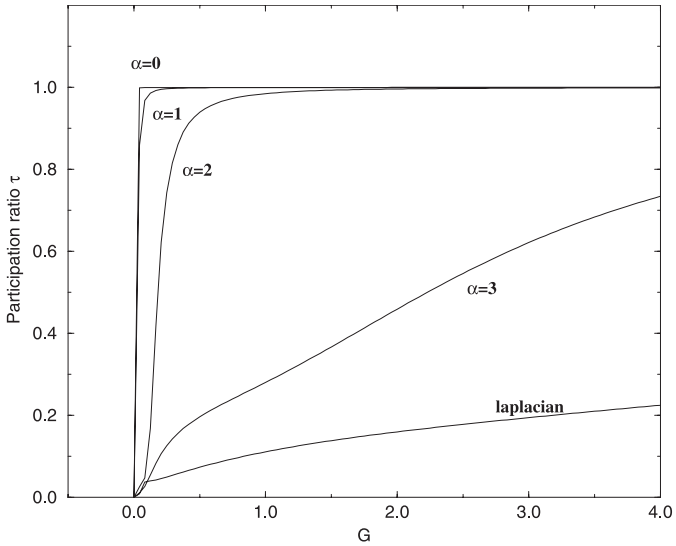

Fig. 3. Participation ratio versus dimensionless surface tension G. The peak in the derivative indicate the critical value G_c of the transition from strong to weak pinning.

Moreover, the average value of G_c also depends on the system size. We have plotted in Figure 5 the average value of G_c. The error bars correspond to the variance of the distribution. This figure can be seen as a phase diagram. It allows us to separate two phases. For a given dimensionless surface tension G, the system can go from one pinning regime to the other when increasing its size. For example, when $\alpha < 1$, the pinning is *weak* for large sizes and *strong* for small sizes. When $\alpha > 1$, the pinning is *strong* for large sizes, and *weak* only for small sizes. We can thus define a critical length $L_t(G)$, below which the pinning is weak, and beyond which the pinning becomes strong. Equivalently, for a given size N the pinning is weak at large $G > G_c$ and strong elsewhere. It is interesting to mention that, for a given G and very large systems, the pinning is weak if the couplings are long range ($\alpha \leq 1$), but it is *strong* if the couplings are short range. The critical value $\alpha_c = 1$ is different from the value below which disorder would be irrelevant after renormalisation ($\alpha_c = 1.5$) [16,18,19]. This difference could be explained by the fact that we do not take into account here the cumulative effect of disorder during the motion of the system. We can indeed propose a qualitative explanation to understand the scaling law $G_c(L)$ of the separation between the two regimes.

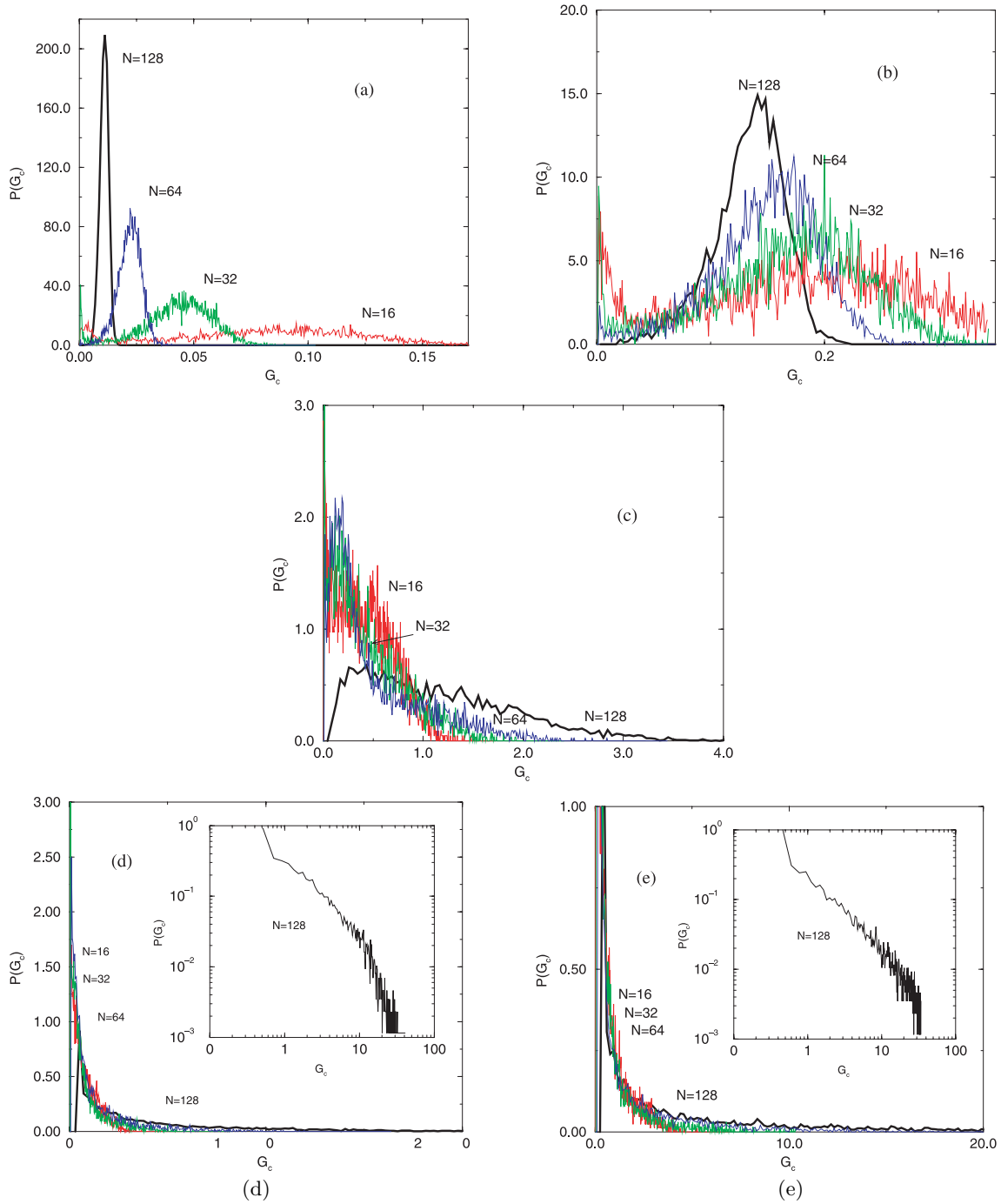

Fig. 4. Distribution of the critical value G_c of the transition. (a): For $\alpha = 0$ and $N = 16, 32, 64, 128$. (b): For $\alpha = 1$ and $N = 16, 32, 64, 128$. (c): For $\alpha = 2$ and $N = 16, 32, 64, 128$. (d): For $\alpha = 3$ and $N = 16, 32, 64, 128$. (e): For nearest neighbour couplings, same sizes. The thick black lines correspond to the largest size $N = 128$.

In Figure 5, the size dependence of the critical G_c seems in agreement with the scaling law

$$G_c \propto L^{\alpha-1}. \tag{13}$$

This can be explained by comparing the pinning energy on each site ($V_p \propto Wd^2$) with the long wavelength contribution to the elastic energy on each site ($V_{el} \propto \gamma d^2 (L/d)^{1-\alpha}$ for a typical distortion of size d, and wavelength L/d). When $\alpha \leq 1$, the *elastic* energy dominates at large scales and pinning is weak. When $\alpha > 1$, the *pinning* energy dominates at large scales: pinning is strong. By comparing V_p to V_{el}, we get the scaling of the critical surface tension G_c, equation (13), in agreement with the qualitative behaviour observed numerically in Figure 5. In case of nearest neighbour couplings, we can compare this criterion to the Anderson criterion of localization as presented

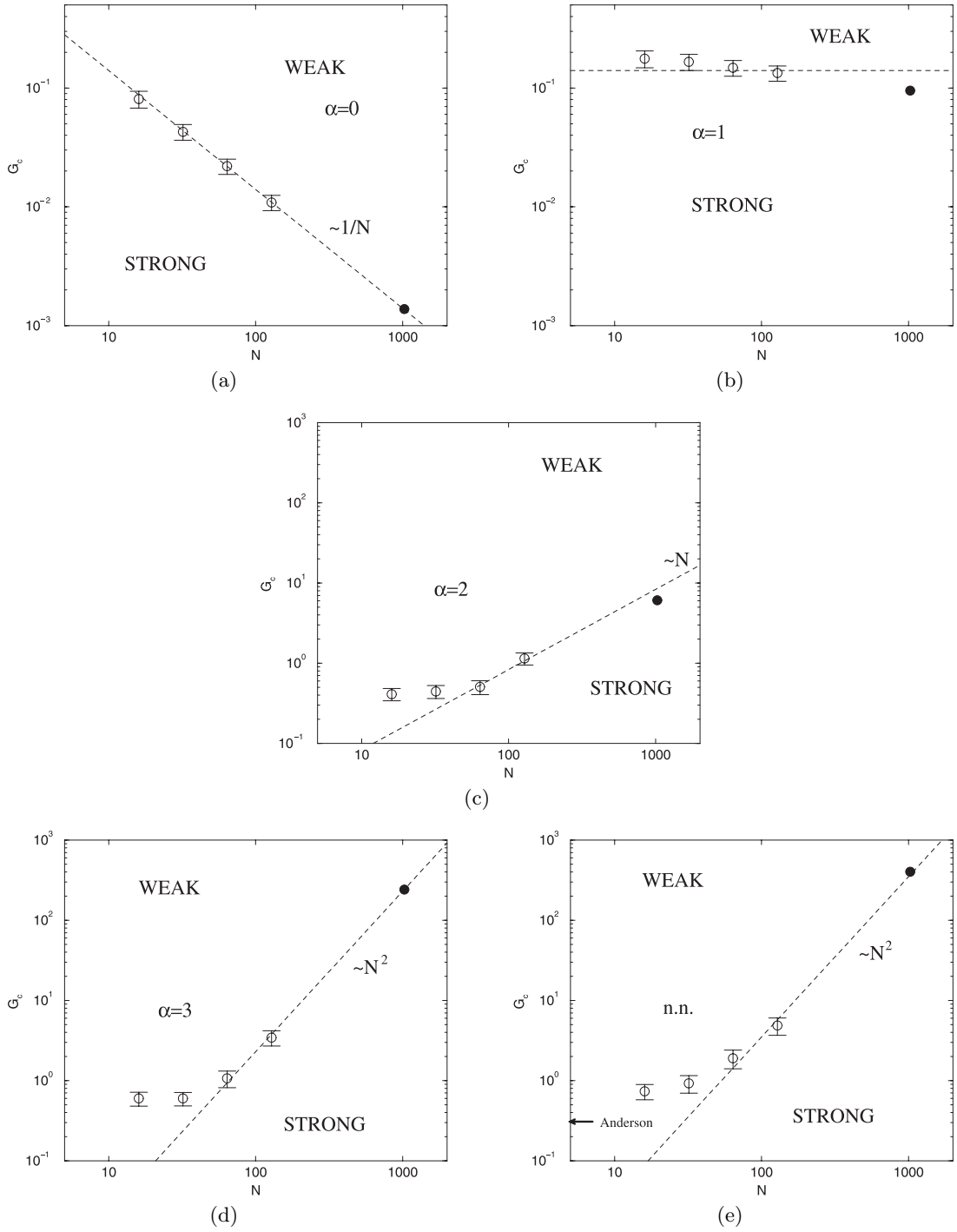

Fig. 5. Average critical value G_c of the surface tension as a function of the system size for $\alpha = 0, 1, 2, 3$, nearest neighbour couplings. The error bars correspond to the variance of the distribution. The point for $N = 1024$ has been obtained with an average over only 100 configurations. The dashed line is a fit $\propto N^{\alpha-1}$.

by Ziman in his book [38]: $G < 1/4e$. There is no size dependence in the Anderson criterion. It appears to underestimate the average value of G_c that we have obtained numerically in our system, as can be seen in Figure 5e.

To further characterize the transition, we have studied more precisely the shape $\delta U(x)$ of the front in each side of the transition. Figure 6a shows the normalized velocity field of the instability in the *strong* pinning case. In this case, it is possible to define a characteristic length along the front by studying the correlation function of the velocity field

$$C(r) \equiv \langle \delta U(0) \delta U(r) \rangle_0.$$

Some correlation functions are presented in Figure 7 for $G < G_c$. When $G \ll G_c$, $C(r)$ decays exponentially. It is thus possible to define a characteristic correlation

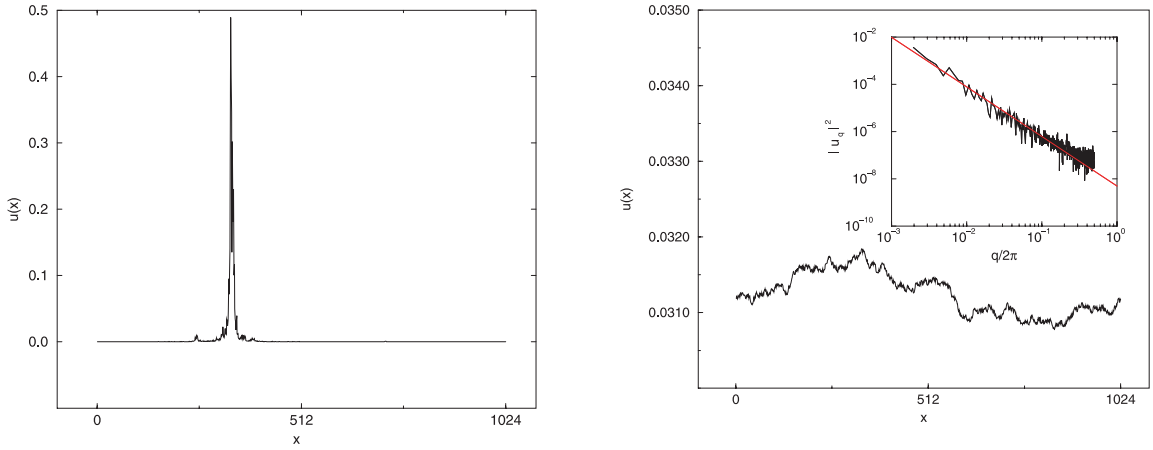

Fig. 6. Examples of displacement field for $L = 1024$ and $\alpha = 2$. Left (a): in the strong pinning regime ($G/G_c = 0.1$). The front is correlated over a length L_c (see Fig. 7). Right (b): In the weak pinning regime ($G/G_c = 100$). The front is rough. It advances as a whole. Inset: Log-log plot of the power spectrum of the displacement field in this case, averaged over 10 configurations. The slope is -2. It corresponds to a roughness exponent $\zeta = 0.5$ for $\alpha = 2$.

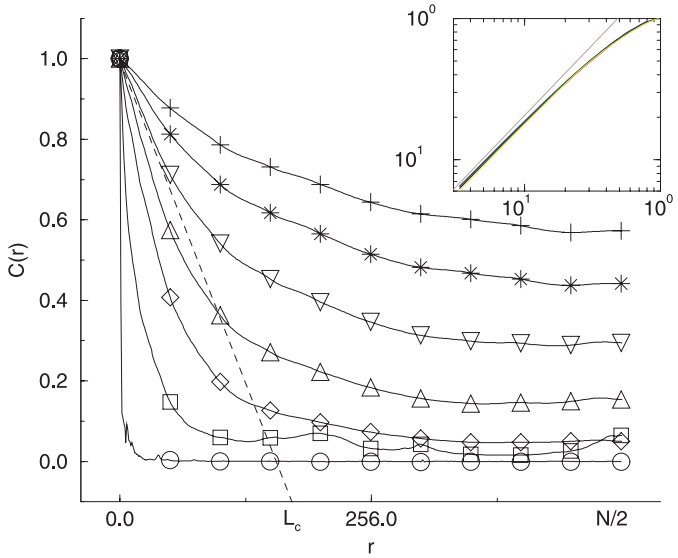

Fig. 7. Normalized correlation function $C(r) \equiv \langle u(r) \cdot u(0)\rangle_0 / \langle u(0)^2\rangle_0$ of the displacement front for various dimensionless surface tension $G/G_c = 1/30, 1/6, 1/3, 1/2, 2/3, 5/6, 1$. Here with $\alpha = 2$ and $L = 1024$. Inset: Correlation length L_c- defined by the slope at the origin $r = 0$ of $C(r)$ in the strong pinning regime versus surface tension G, for $L = 1024$ and $\alpha = 2, 2.25, 2.5, 2.75, 3$. Here both quantities have been normalized as $(L_c^* - L_c)/L_c^*$ for the vertical axis and $(G_c - G)/G_c$ for the horizontal axis. $L_c^*(\alpha, L)$ is the correlation length at $G = G_c$. It can be seen that all curves for $2 < \alpha < 3$ superimpose.

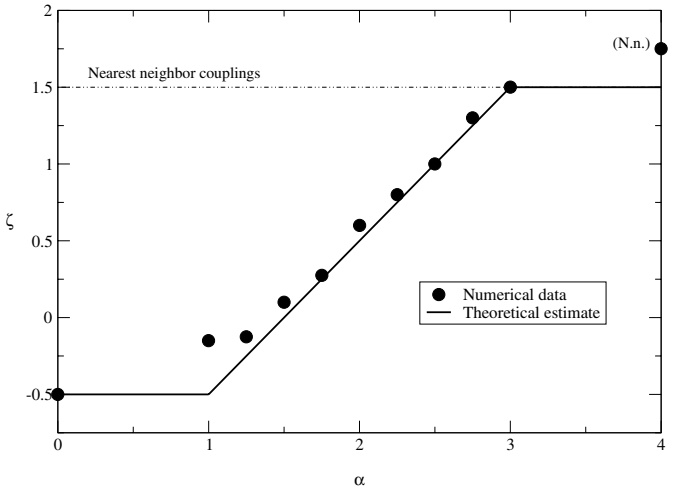

Fig. 8. Roughness exponent ζ, in the weak pinning regime, versus the range of coupling α. The line corresponds to the theoretical estimate obtained in three different regions: $\zeta = (2\alpha - 3)/2$ for $1 < \alpha < 3$, $\zeta = -0.5$ (white noise) for $\alpha < 1$, and $\zeta = 1.5$ for $\alpha > 3$. There are logarithmic corrections, not mentioned in this figure, in the theoretical estimate for α close to 1, and α close to 3.

length L_c by the slope of the tangent to $C(r)$ at the origin $r = 0$. When $G \to G_c^-$, L_c tends to a finite value L_c* of the order of the system size. The inset in Figure 7 shows that L_c depends linearly on the surface tension G. Together with the scaling of equation (13), we thus obtain the scaling $L_c \propto L_c^*(L) G(L/d)^{1-\alpha}$ for the correlation length.

The correlation function $C(r)$ is quite different in the *weak* pinning case. In this case, as soon as $G > G_c$, the power spectrum of $\delta U(x)$ displays a characteristic power law behaviour that prohibits us from defining any characteristic length along the front (despite d and L). It is only possible to define a *roughness exponent* ζ such as

$$C(r) \propto r^{2\zeta}. \tag{14}$$

Figure 8 shows the dependence of ζ (measured in the power spectrum of δU) on the range of the couplings, α. The continuous line corresponds to a perturbative calculation that we will discuss now in the following section.

4 Weak pinning

In the weak pinning regime it is possible to perform a perturbative calculation. The instability problem consists of the diagonalization of a random dynamical matrix, and the perturbative calculation is analogous to that used in quantum mechanics [40]. In order to perform the perturbative calculation (see Appendix A) we separate the average contribution to the dynamical matrix $\mathcal{A}$ and the fluctuating contribution due to disorder. This method is justified in the *weak* pinning case by the fact that the front advances mainly as a whole. (It is quite different from the perturbative calculation performed in [24] where the off-diagonal elastic terms of $\mathcal{A}$ are used as perturbative parameter.) Here, the small parameter of the perturbation is the variance W of the disorder terms (in agreement with the condition $G \gg G_c$). The dynamical matrix $\mathcal{A}$ is separated into an average part $\mathcal{A}_0$ (Eq. (23)) and a diagonal part $\mathcal{A}_1$ (Eq. (24)) containing all of the X_i,

$$X_i \equiv V_p''(x_i^0) - \langle V_p'' \rangle \tag{15}$$

in the diagonal. The eigenvector $u_o(x)$ corresponding to the smallest eigenvalue of $\mathcal{A}_0$ is well known: it corresponds to the translational invariance of $\mathcal{A}_0$, $u_0(x_i) \equiv u$, with the eigenvalue

$$\eta\omega_0 = \langle V_p'' \rangle + K_{ext}.$$

The perturbative calculation allows us to easily obtain the first corrections to the eigenvector and the eigenvalue. At first order, we obtain the correction to the eigenvector via the equation

$$\mathcal{G} \int_d^L dx' \frac{u_1(x) - u_1(x')}{|x - x'|^\alpha} = u \left(\langle V_p'' \rangle - V_p''(x) \right) \tag{16}$$

which can be solved in the Fourier space (with periodic boundary conditions)

$$\tilde{u_1}(q) = \frac{-u}{4\mathcal{G}} \frac{\tilde{V_p''}(q) q^{1-\alpha}}{\int_{qd}^{qL} dv \, \sin^2(v/2)/v^\alpha}. \tag{17}$$

This result allows us (Appendix. A.2) to compute the roughness exponent of $\delta U(x)$. In the case of a uncorrelated disorder of zero mean, with $\left\langle V_p''(x) V_p''(x') \right\rangle = W^2 \delta(x - x')$, we get

$$\begin{aligned} \zeta &= (2\alpha - 3)/2 \text{ for } 1 < \alpha < 3 \\ \zeta &= -0.5 \text{ when } \alpha < 1 \\ \text{and } \zeta &= 1.5 \text{ when } 3 < \alpha. \end{aligned} \tag{18}$$

This estimate is shown in Figure 8. It is in very good agreement with the results of the numerical simulations. It is also in agreement with the calculation of Larkin et al. [22,25], as equation (16) is indeed an equilibrium equation relating the elastic forces to a linear approximation of pinning forces. Note however that in our case, there is no correlation length at all along the front in the weak pinning regime. In order to compare the *Larkin criterion* of multistability and the criterion of instability given in equation (11), we need to compute the relaxation time $1/\omega$.

The calculation of the eigenvalue ω needs a second order calculation (Appendix A.3). At the second order we get

$$\omega = \omega_0 + \omega_2 \tag{19}$$

with

$$\langle \omega_2 \rangle = \left\langle \frac{-1}{\eta\mathcal{G}} \int_0^{+\infty} \frac{dq}{4\pi} \frac{L |\tilde{V_p''}(q)|^2 q^{1-\alpha}}{\int_{qd}^{qL} dv \, \sin^2(v/2)/v^\alpha} \right\rangle \propto \frac{-W}{\eta G} f(N) \tag{20}$$

where the brackets indicate average over disorder. The instability criterion which corresponds to $\omega < 0$ is always favoured by the second order term (since $\omega_2 < 0$). It means that the disorder is always in favor of instability. Moreover, we can study the size dependence of $\langle \omega_2 \rangle$ through the function $f(N)$ in equation (20). This is done numerically in Figure 9 for various couplings α. In each case, we see a very good agreement with the perturbative calculation (for more details see Appendix A.3). Note that the size dependence of $\langle \omega_2 \rangle$ has not the same consequences when the couplings are short range, or long range. For long range couplings ($\alpha \leq 1$), the average absolute value $|\omega_2|(N)$ decreases: the system is stabilized when its size increases. For short range couplings on the contrary ($\alpha > 1$), $|\omega_2|(N)$ increases, leading to systems that become unstable at large sizes. This is the case of wetting for example. In this case, collective effects may be responsible for the destabilization of the contact line at large scales ($L > L_s$), even if the system is locally monostable. This is qualitatively in agreement with the collective instabilities mentioned in references [22–25]. Note however that in our case the instability criterion ($\omega < 0$) does not give the same scaling as the Larkin criterion $\langle u^2 \rangle^{1/2} \geq a$, and is neither related to any correlation length along the front.

5 Conclusion

The linear stability analysis of our system is a way to show the change from the weak to the strong pinning regimes. It immediately generalizes to a deformable line with many defects, the well known mean-field criterion of multistability which is valid only for a very rigid system or in a single defect approximation [18,19,22,23]. Moreover, a small disorder perturbative calculation completes our study in the weak pinning regime. Our approach allows thus to underline precisely the role of disorder. There are analogies between the "weak to strong pinning" transition shown here and the well known localization transition in one dimension [38,39]. However, our systematic numerical study allows us to point out the role of the size of the system, and the role of the long range of elastic couplings. This has never been shown before.

We have shown for example (Sects. 3–4) that systems with long-range interactions ($\alpha \leq 1$) have a qualitatively different behaviour than systems with shorter range interactions ($\alpha > 1$). When the interactions are long-range

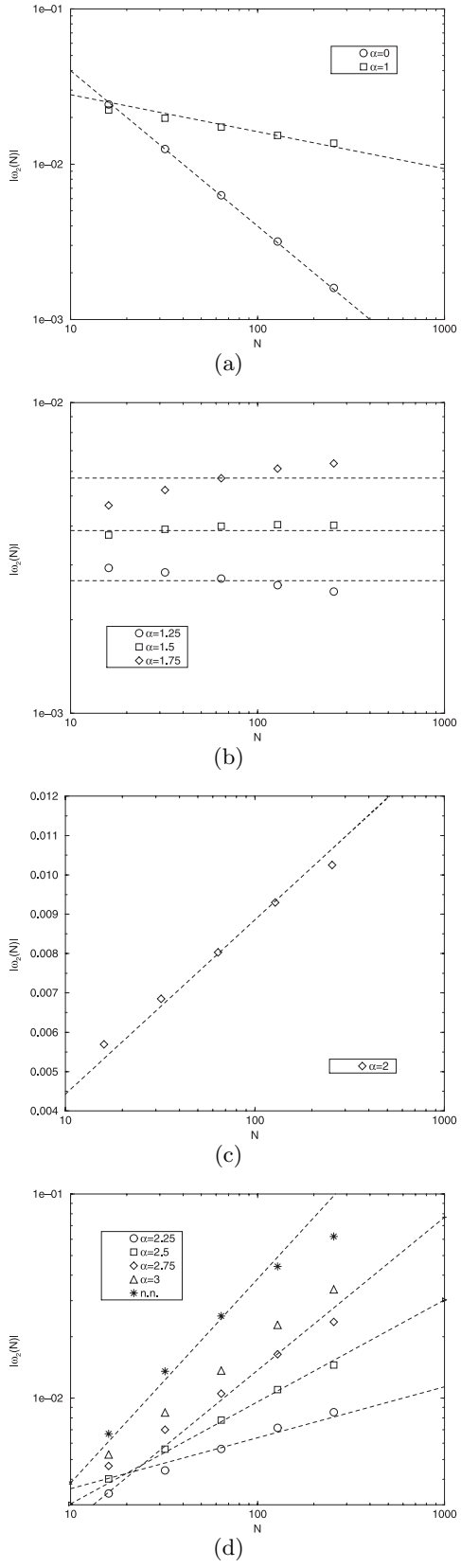

Fig. 9. $|\omega_2|$ as a function of the system size for $\alpha = 0, 1$ (a) $\alpha = 1.25, 1.5, 1.75$ (b) $\alpha = 2$ (c) $\alpha = 2.25, 2.5, 2.75, 3$, nearest neighbour couplings, in the weak pinning regime. Dashed lines correspond to the theoretical estimate discussed in the text.

($\alpha \leq 1$), the large scale behaviour of the system belongs to the weak pinning regime, and large size systems are more stable. In contrast, when the interactions are short-range ($\alpha > 1$), the large scale behaviour of the system belongs to the strong pinning regime, and large size systems may display collective instabilities (Sect. 4). This can be qualitatively understood by the fact that elastic energy dominates at large scales when $\alpha \leq 1$, but pinning energy dominates at large scales when $\alpha > 1$.

For a given disorder W and a given surface tension γ, we have shown (see Sect. 3) the existence of a critical length L_t separating a weak pinning regime and a strong pinning regime. Conversely, for a given system size, it is possible to define a critical dimensionless "surface tension to disorder" ratio, G_c, below which the system is strongly pinned, and above which it is weakly pinned. However, the determination of G_c and its error bar depends on the system size, and it may be difficult to get a priori an experimental value for G_c. We have shown in this paper another way to characterize the change from the strong pinning regime to the weak pinning regime. Experimentally, it is easier to characterize each regime by the relaxational behaviour of a line to its equilibrium position. We have shown in this paper, that when the system is strongly pinned, its velocity field is correlated over a length $L_c \propto G$. In contrast, when the front is weakly pinned, it advances as a whole. In this case, there is no characteristic length along the front but the power spectrum allows one to measure a roughness exponent whose value is in agreement with the perturbative calculation ($\zeta \approx (2\alpha - 3)/2$).

The *weak* pinning regime is equivalent to the regime studied by Larkin et al. [22]. In this case, the roughness exponent ζ characterizing the relaxation process is the same as the roughness exponent characterizing the equilibrium position of an initially flat line [13,22]. However, in our case, there is no characteristic length along the front in the weak pinning regime. Moreover, the *Larkin criterion* of multistability $\langle u^2 \rangle^{1/2} \propto a$ (where a is the typical size of a defect) do not yield the same scaling as our second order computation of the relaxation time. The last one is directly related to the stability of the system. At this stage, the Larkin criterion thus seems to be artificially constructed and may call for more thorough study.

In the *strong* pinning regime, we have shown the existence of a correlation length L_c in the relaxation mode of the front. We could ask whether this length L_c is analogous to the length L_t below which the system is weakly pinned. In case of wetting (with $\alpha = 2$), both lengths coincide ($L_c \approx L_t \propto G$). In this particular case, the motion of the system could thus be described as weakly pinned blocks of size L_c. In other cases, the scalings of $L_c(G)$ and $L_t(G)$ are different. However, we do not know how the correlation length L_c evolves when the system reaches its quasistatic stationary state. Further numerical work is now in progress to answer this question.

Let us note finally that the roughness exponent found in the weak pinning regime ($\zeta = 0.5$ in case of wetting) is larger than those reported in references [18,19,31] in the strong pinning regime ($\zeta \approx 0.33$). The latter has

$$\underline{\underline{\mathcal{A}}} \equiv \begin{pmatrix} K_{ext} + V_p''(u_{eq}(x_1)) + g_{12} + ... + g_{1N} & & -g_{ij} \\ & \ddots & \\ -g_{ij} & & K_{ext} + V_p''(u_{eq}(x_i)) + g_{N1} + ... + g_{NN-1} \end{pmatrix}$$

$$\mathcal{A}_0 = \begin{pmatrix} K_{ext} + \langle V_p'' \rangle + g_{12} + ... + g_{1N} & & -g_{ij} \\ & \ddots & \\ -g_{ij} & & K_{ext} + \langle V_p'' \rangle + g_{N1} + ... + g_{NN-1} \end{pmatrix} \quad (23)$$

been obtained within numerical simulations or one-loop renormalisation. The former is closer to experimental results [1,2,9]. Two-loop renormalisation [16] on the same system gives a roughness exponent closer to the weak pinning regime.

In both the weak and the strong pinning regimes, temperature could play a crucial role in the choice of an equilibrium state and thus on the morphology of the front in a stationary state. This has already been mentioned by Chudnovsky et al. [41], who have studied the dependence of the equilibrium state on the damping rate. This could explain the origin of the characteristic length obtained along the front by Hazareesing et al. [20] (using statistical averages) and by Bocquet et al. [27] (by molecular dynamics, at very small but non zero temperature). The relationship between this length and the length L_t is still unclear. Another natural way to extend our study would be to focus not only on the *most* unstable mode, but on all the relaxation modes and on their density. Due to the superposition of the relaxation modes, the system could display a characteristic length at zero temperature, even in the weak pinning regime. This should also clarify how the phase space is explored during the deterministic motion of the system. Finally, our work allows one to define precisely a weak and a strong pinning regime and the transition between them. The study of the motion of the system beyond instability should now provide interesting results on the stationary state and on the associated dissipated energy, in both pinning regimes.

We are thankful to J. Crassous, P. LeDoussal, E. Rolley, S. Roux for very useful discussions.

Appendix A: Perturbative theory

A.0. In this appendix, we show how to solve the linear equation

$$\underline{\underline{\mathcal{A}}} \delta U(x) = \eta \omega \delta U(x) \quad (21)$$

using a small disorder perturbation theory, in a system with periodic boundary conditions. In our model,

see equation above

g_{ij} is the long range elastic stiffness, with periodic boundary conditions

$$g_{ij} \equiv \frac{\mathcal{G}d}{|x_i - x_j|^\alpha} + \frac{\mathcal{G}d}{|x_i - x_j - L|^\alpha} \quad (22)$$

$\underline{\underline{\mathcal{A}}}$ is split into two parts

$$\underline{\underline{\mathcal{A}}} = \mathcal{A}_0 + \mathcal{A}_1$$

with the zeroth order, average part

see equation (23) above

and the first order, random diagonal part

$$\mathcal{A}_1 = \begin{pmatrix} V_p''(u_{eq}(x_1)) - \langle V_p'' \rangle & & 0 \\ & \ddots & \\ 0 & & V_p''(u_{eq}(x_N)) - \langle V_p'' \rangle \end{pmatrix}. \quad (24)$$

Here, $\langle V_p'' \rangle \equiv \int_0^L dx/L V_p''(x)$ is the average pinning.

The perturbation theory consists in expanding the linear equation (21) at successive orders

$$(\mathcal{A}_0 + \mathcal{A}_1)(u_0 + u_1 + u_2 + \cdots) = \eta(\omega_0 + \omega_1 + \omega_2 + \cdots)(u_0 + u_1 + u_2 + \cdots)$$

and comparing each term order by order.

A.1. We get, **at zero order**, $\mathcal{A}_0 u_0 = \eta \omega_0 u_0$ with

$$u_0 \propto u. \begin{vmatrix} 1 \\ 1 \\ . \\ . \\ . \\ 1 \end{vmatrix}, \text{ and } \omega_0 = K_{ext} + \langle V_p'' \rangle.$$

A.2. The **first order** calculation provides the roughness exponent of the front. Multiplying

$$\mathcal{A}_0 u_1 + \mathcal{A}_1 u_0 = \eta(\omega_0 u_1 + \omega_1 u_0)$$

by ${}^t u_0$, and using Riemann summation, we get

$$\omega_1 = \frac{{}^t u_0 \mathcal{A}_1 u_0}{{}^t u_0 u_0} \approx \frac{\int_d^L dx \, \left(V_p''(x) - \langle V_p'' \rangle\right)}{\int_d^L dx} = 0. \quad (25)$$

The remaining equation ($(\mathcal{A}_0 - \eta\omega_0)u_1 = -\mathcal{A}_1 u_0$) yields, for each site x:

$$\mathcal{G}\int_{|x-x'|\geq d}^{L} dx'\ (u_1(x) - u_1(x')) \times \left(\frac{1}{|x-x'|^\alpha} + \frac{1}{(L-|x-x'|)^\alpha}\right) = \left(\left\langle V_p''\right\rangle - V_p''(x)\right) u \quad (26)$$

which can be solved using the following Fourier Transform:

$$\tilde{u}(q) \equiv \int_0^L \frac{dx}{L}\, u(x) e^{-iq.x}$$
$$\text{and}\ \ u(x) = \int_0^{+\infty} \frac{dqL}{2\pi}\, \tilde{u}(q) e^{+iq.x}.$$

The Fourier Transform of (26) yields

$$\tilde{u_1}(q) = \frac{\left(\tilde{V}''(0) - \tilde{V}''(q)\right) u}{2\mathcal{G} q^{\alpha-1} \int_{q.d}^{q.L} dv\, \frac{1-\cos v}{v^\alpha}} \quad (27)$$

because

$$\int_{|x-x'|\geq d}^{L} dx' \left(1 - e^{iq.(x-x')}\right) \times \left(\frac{1}{|x-x'|^\alpha} + \frac{1}{(L-|x-x'|)^\alpha}\right) = 2\int_{r=d}^{L} dr\, \frac{1-\cos(qr)}{r^\alpha}. \quad (28)$$

In case of a uncorrelated disorder,

$$\left\langle \left(V_p''(x) - \left\langle V_p''\right\rangle\right)\left(V_p''(x') - \left\langle V_p''\right\rangle\right)\right\rangle = W^2\delta(x-x') \Longrightarrow \left\langle \left|\tilde{V}''(q) - \tilde{V}''(0)\right|^2 \right\rangle = \frac{d}{L} W^2, \quad (29)$$

and using the approximation

$$1 - \cos v = 2\sin^2\left(\frac{v}{2}\right) \approx \frac{v^2}{2} \text{ if } \frac{v}{2} \ll 1 \text{ and } \approx 1 \text{ elsewhere,} \quad (30)$$

we get from (27) the average Fourier coefficients of the first order displacement field:

$$< |\tilde{u_1}(q)|^2 > \propto \frac{u^2 W^2}{\mathcal{G}^2}\frac{d}{L}(qd)^{2-2\alpha} \ \propto q^{-1-2\zeta}\ \ 1 < \alpha < 3$$
$$\propto \frac{u^2 W^2}{\mathcal{G}^2}\left(\frac{L}{d}\right)^{2\alpha-3} \quad \alpha < 1\ \zeta = -0.5$$
$$\propto \frac{u^2 W^2}{\mathcal{G}^2}\frac{d}{L}(qd)^{-4} \quad \alpha > 3\ \zeta = 1.5$$

with logarithmic corrections when $\alpha = 1$ and $\alpha = 3$. For $1 < \alpha < 3$, the roughness exponent $\zeta = (2\alpha - 3)/2$.

A.3. The **second order** calculation allows one to compute the second order correction to the relaxation time.

From

$$\mathcal{A}_0 u_2 + \mathcal{A}_1 u_1 = \eta(\omega_0 u_2 + \omega_1 u_1 + \omega_2 u_0)$$

multiplied by ${}^t u_0$, with equation (25), we get

$$\eta\omega_2 = \frac{{}^t u_0 \mathcal{A}_1 u_1}{{}^t u_0 u_0}.$$

Using equation (27) we get

$$\eta\omega_2 = -\frac{1}{2\mathcal{G}}\int_0^{+\infty} \frac{dq}{2\pi} \frac{q^{1-\alpha}\left|\tilde{V}''(q) - \tilde{V}''(0)\right|^2}{\int_{qd}^{qL} dv\, \frac{1-\cos v}{v^\alpha}}.$$

Thus finally, with the approximation (30) and in case of decorrelated disorder (29) we get the average value

$$\begin{aligned}
\langle\omega_2\rangle &\propto -\frac{W^2}{\eta\mathcal{G}}\frac{1-\alpha}{2}L^{\alpha-1} \text{ for } \alpha < 1\\
\langle\omega_2\rangle &\propto -\frac{W^2}{\eta\mathcal{G}}\frac{(3-\alpha)(\alpha-1)(2\pi)^{1-\alpha}}{2^{2-\alpha}(1+\alpha)(2-\alpha)}d^{\alpha-1} \text{ for } 1 < \alpha < 2\\
\langle\omega_2\rangle &\propto -\frac{W^2}{\eta\mathcal{G}}\frac{(3-\alpha)(\alpha-1)(2\pi)^{1-\alpha}}{2^{2-\alpha}(1+\alpha)(\alpha-2)}dL^{\alpha-2} \text{ for } 2 < \alpha < 3\\
\langle\omega_2\rangle &\propto -\frac{W^2}{\eta\mathcal{G}}\frac{2(\alpha-3)}{8\pi^2}d^{\alpha-2}L \text{ for } 3 < \alpha.
\end{aligned} \quad (31)$$

References

1. J. Schmittbuhl, S. Roux, J.-P. Vilotte, K.J. Maloy, Phys. Rev. Lett. **74**, 1787 (1995)
2. E. Bouchaud, J. Phys.: Condens. Matter **9**, 4319 (1997) For a large review, see *Physical Aspects of Fracture*, edited by E. Bouchaud et al. (NATO science study, September 2001)
3. J.F. Joanny, P.G. de Gennes, J. Chem. Phys. **81**, 552, (1984)
4. P.G. de Gennes, Rev. Mod. Phys. **57**, 827 (1985)
5. Y. Pomeau, J. Vannimenus, J. Colloid Interface Sci. **104**, 477 (1985)
6. J. Crassous, E. Charlaix, Europhys. Lett. **28**, 415 (1994)
7. J.-M. di Meglio, Europhys. Lett. **17**, 607 (1992)
8. S. Ramos, E. Charlaix, A. Benyagoub, M. Toulemonde, Phys. Rev. E **67**, 031604 (2003)
9. E. Rolley, C. Guthmann, R. Gombrowivz, V. Repain, Phys. Rev. Lett. **80**, 2865 (1998)
10. A. Prevost, E. Rolley, C. Guthmann, Phys. Rev. B **65**, 064517 (2002)
11. S. Moulinet, C. Guthmann, E. Rolley, Eur. Phys. J. E **8**, 437 (2002)
12. T. Cubaud, *Thèse de l'université Paris XI* (2001); T. Cubaud, M. Fermigier, Europhys. Lett. **55**, 239 (2001)
13. J.F. Joanny, M.O. Robbins, J. Chem. Phys. **92**, 3206 (1990); M.O. Robbins, J.F. Joanny, Europhys. Lett. **3**, 729 (1987)

14. R. Golestanian, E. Raphael, Phys. Rev. E **67**, 031603 (2003)
15. A. Rosso, W. Krauth, Phys. Rev. Lett. **87**, 187002 (2001); A. Rosso, W. Krauth Phys. Rev. E **65**, 025101(R) (2002); A. Rosso, A.K. Hartmann, W. Krauth, Phys. Rev. E **67**, 021602 (2003); A. Rosso, W. Krauth, P. Le Doussal, J. Vannimenus, K.J. Wiese, `cond-mat/0301464`
16. P. Le Doussal, K.J. Wiese, P. Chauve, Phys. Rev. B **66**, 174201 (2002); P. Le Doussal, K.J. Wiese, Phys. Rev. E **67**, 016121 (2003); P. Le Doussal, K.J. Wiese, `cond-mat/0301465`. P. Le Doussal, K.J. Wiese, P. Chauve, `cond-mat/0304614`
17. T. Nattermann et al., J. Phys. II France **2**, 1483 (1992)
18. D.S. Fisher, Phys. Rev. B **31**, 1396 (1985)
19. D. Ertas, M. Kardar, Phys. Rev. B **53**, 3520 (1996)
20. A. Hazareesing, M. Mézard, Phys. Rev. E **60**, 1269 (1999)
21. S. Zapperi, P. Ciseau, G. Durin, E. Stanley, Phys. Rev. B **58**, 6353 (1998)
22. A.I. Larkin, Y.N. Ovchinnikov, J. Low Temp. Phys. **34**, 409, (1979); For a review, see T. Giamarchi, P. Le Doussal, *in Spin Glasses and Random fields*, edited by A.P. Young, (World Sci., Singapore,1997)
23. C. Caroli, P. Nozières, *in The physics of sliding friction*, edited by B.N.J. Persson, Vol. 311 of NATO Advanced Study (Kluwer, Dordrecht, 1996)
24. C. Caroli, P. Nozières, Eur. Phys. J. B **4**, 233 (1998)
25. B.N.J. Persson, *Sliding Friction (Physical Principles and Applications)* (Springer-Verlag, Heidelberg, 1998)
26. R. Burridge, L. Knopoff, Bull. Seismol. Soc. Am. **57**, 341 (1967)
27. L. Bocquet, H.J. Jensen, J. Phys. I France **7**, 1603 (1997)
28. A. Tanguy, Thèse de l'université Paris VII (1998)
29. S. Krishnamurthy, A. Tanguy, P. Abry, S. Roux, Europhys. Lett. **51**, 1 (2000)
30. S. Krishnamurthy, A. Tanguy, S. Roux, Eur. Phys. J. B **15**, 149 (2000)
31. A. Tanguy, M. Gounelle, S. Roux, Phys. Rev. E **58**, 1577 (1998)
32. L.-H. Tang et al., Phys. Rev. Lett. **74**, 920 (1995); M. Kardar, Phys. Rep. **301**, 85 (1998); P. Le Doussal, K.J. Wiese, Phys. Rev. E **67**, 016121 (2003)
33. A. Paterson et al., Phys. Rev. E **51**, 1291 (1995) A. Paterson, M. Fermigier, Phys. Fluids **9**, 2210 (1997)
34. Let us recall that, in the context of this paper, temperature is zero. Thus an *equilibrium* position is simply one of the configurations of the contact line, where the sum of forces acting on the line, is equal to zero
35. `http://www.netlib.org/eispack`
36. `http://www.caam.rice.edu/software/ARPACK/`
37. We have checked that this kind of distribution corresponds precisely to the distribution of pinning forces along the chain when it reaches its *first* equilibrium position: using conjugated gradient method, we have quenched very quickly a chain initially flat on a random surface. When the disorder on the surface, here the amplitude of the pinning centers, is decorrelated, the disorder along the chain at equilibrium is also decorrelated. The morphology of the line is not the same in the strong or in the weak pinning regime. The roughness exponent of the chain at equilibrium in the weak pinning regime is $\zeta = (2\alpha - 3)/2$ as found already by Larkin et al. [22,25]. A. Tanguy and T. Vettorel, in preparation (2003)
38. J.M. Ziman *Models of disorder* (Cambridge university press, Cambridge, 1979)
39. J.-M. Luck, *Systèmes désordonnés unidimensionnels* (Aléa Saclay, Gif-sur-Yvette, 1992)
40. C. Cohen-Tannoudji, B. Diu, F. Laloë *Mécanique Quantique*, tome II (Hermann, Paris, 1973)
41. E.M. Chudnovsky, R. Dickman, `cond-mat/9710184`